

The C₆₀-Fullerene Porphyrin Adducts for Prevention of the Doxorubicin-Induced Acute Cardiotoxicity in Rat Myocardial Cells

Seyed Vahid Shetab Boushehri¹, Seyed Nasser Ostad^{1*}, Saeed Sarkar², Dmitry A. Kuznetsov³, Anatoly L. Buchachenko⁴, Marina A. Orlova, Bagher Minaii⁵, Abbas Kebriaeezadeh¹, and Seyed Mahdi Rezayat⁶

¹ Department of Toxicology and Pharmacology, Faculty of Pharmacy & Nanotechnology Research Center, Tehran University of Medical Sciences, Tehran, Iran

² Research Center for Science and Technology in Medicine (RCSTIM), Tehran University of Medical Sciences, Tehran, Iran

³ N.N. Semenov Institute for Chemical Physics, Russian Academy of Sciences, Moscow, Russian Federation

⁴ Department of Chemistry, M.V. Lomonosov Moscow State University, Moscow, Russian Federation

⁵ Department of Anatomy, School of Medicine, Tehran University of Medical Sciences, Tehran, Iran

⁶ Department of Medical Nanotechnology, Tehran University of Medical Sciences, Tehran, Iran

Received: 26 Dec. 2008; Received in revised form: 29 Apr. 2009; Accepted: 28 Jun. 2009

Abstract—This is a fullerene-based low toxic *nanocationite* designed for targeted delivery of the paramagnetic stable isotope of magnesium to the doxorubicin (DXR)-induced damaged heart muscle providing a prominent effect close to about 80% recovery of the tissue hypoxia symptoms in less than 24 hrs after a single injection (0.03 – 0.1 LD₅₀). Magnesium magnetic isotope effect selectively stimulates the ATP formation in the oxygen-depleted cells due to a creatine kinase (CK) and mitochondrial respiratory chain-focusing “attack” of ²⁵Mg²⁺ released by nanoparticles. These “smart nanoparticles” with membranotropic properties release the overactivating cations *only* in response to the intracellular acidosis. The resulting positive changes in the energy metabolism of heart cell may help to prevent local myocardial hypoxic (ischemic) disorders and, hence, to protect the heart muscle from a serious damage in a vast variety of the hypoxia-induced clinical situations including DXR side effects.

© 2010 Tehran University of Medical Sciences. All rights reserved.
Acta Medica Iranica 2010; 48(5): 342-350.

Key words: Fullerene nanoparticles, doxorubicin-induced cardiotoxicity, ²⁵Mg²⁺, mitochondrial dysfunctions.

Introduction

Drug-induce hypoxia, i.e. the drug side effects leading to sharp decrease of oxygen consumption in mammalian tissues, complicates some anticancer chemotherapeutic procedures. Thus, DXR-induced cardiotoxicity relates to suppression of the ADP *oxidative phosphorylation* in respiratory chain of myocardial mitochondria (1-3) in addition to its inhibitory effect on oxygen independent *substrate phosphorylation* pathway of the ATP synthesis (4). That means, the reserve ATP regeneration pathway of CK and respiratory chain-directed ADP phosphorylation, could be chosen as a target for pharmacological impact having an aim to minimize, i.e. to reduce if not even exclude, the DXR side effect in a course (or prior to) the long term cytostatic medication.

Being Mg²⁺-dependent processes, both substrate and oxidative phosphorylation pathways might be activated up to 2.5-fold more efficiently by nano-amounts of ²⁵Mg²⁺, *the only magnetic magnesium isotope*, as compared to non-magnetic ²⁴Mg²⁺ and ²⁶Mg²⁺ isotopes (5-7). A simple “endoosmotic pressure” is to replace one Mg isotope by another (all of them are stable ones) inside the CK active site (8).

This is about *the magnetic isotope effect* of ²⁵Mg²⁺ which is now found to be an essential, *overactivating*, element in the magnesium-dependent ATP production control processes (5-8). It makes a targeted delivery of the above mentioned magnetic isotope (+5/2 nuclear spin, 0.85 Bohr magneton magnetic moment, 10% natural abundance) towards a hypoxia damaged cells/tissues a truly important pharmacological task. Thus, the Mg²⁺-

* **Corresponding Author:** Seyed Nasser Ostad

Department of Toxicology and Pharmacology, Faculty of Pharmacy & Nanotechnology Research Center, Tehran University of Medical Sciences, Tehran, Iran

Tel/Fax: +98 21 66959105, E-mail: ostadnas@sina.tums.ac.ir

exchanging nanoparticles would be an appropriate tool for such a targeting.

To achieve this goal, a low toxic ($LD_{50}=896$ mg/kg, i.v., rats), amphiphilic (430 mg/ml water, pH 7.40), membranotropic and cluster forming 1.8-2.0 nm fullerene- C_{60} based particles were designed (9). This product, which possesses a marked cationite properties (Figure 1), is the iron containing porphyrin monoadduct of a classical buckminster fullerene, *buckminsterfullerene(C_{60})-2-(butadiene-1-yl)-tetra(o- γ -aminobutyryl-o-phthalyl)ferroporphyrin*. Hereafter, we refer it to "Porphylleren-MC16" or, in brief, PMC16 (9).

The present work concerns biochemical/pharmacological study of [^{25}Mg] PMC16 effects in rat myocardium affected by the DXR-induced hypoxia with respect to cationite properties of the new nanomedicine tested. This is a part of the broader research project pronouncing an aim to develop a novel nanopharmacological approach to prevent local tissue hypoxia syndromes (including the DXR promoted cardiotoxicity side effect) by a targeted delivery of $^{25}Mg^{2+}$ cations towards the heart muscle using a porphyrinic-fullerene nanoparticles as the membranotropic Mg^{2+} -releasing carriers.

Patients and Methods

DXR, ATP, ADP, phosphocreatine, creatine, $MgCl_2$, sucrose, all of Analytical Grade, were purchased from Merck Corp. USA. All organic solvents used were kindly supplied by Bio-Rad, Russia. Pure magnesium isotopes were received in a chloride form (96.8% isotopic purity, A grade) from Obninsk Radiochemical Centre, Russia. The same supplier was also responsible for the radioactive materials providing: $^{59}FeCl_2$ (A grade, 910-960 Ci/mmol specific activity), sodium [^{32}P]orthophosphate (A grade, 600-700 Ci/mmol) and [^{32}P]phosphocreatine (A grade, 280-320 Ci/mmol) were used. Creatine kinase (60-80 U/mg protein), nuclease S (100-120 U/mg protein) and RNase A (100-140 U/mg protein) were purchased from Worthington Corp., USA. crystalline bacterial proteinase (Nagarase) was purchased from Sigma Chemical Co.

Wistar Albino Glaxo (WAG/Sto2J strain) mail healthy adult rats (180-220 gms) were kept under a standard diet starved for 24 hrs prior to each experiment. Three animals per one experimental point with following 3-6 repetitions of every measurement were used. A conventional non-parametric statistical treatment (for "n" is equal to or less than 6) was performed using the Sigma Biostat A6 software package to evaluate the sig-

nificance of experiment/control differences. P-values less than 0.05 were considered as significance.

DXR 0.60-0.80 mg/kg i.v. once per 24 hrs was employed for induction of *in vivo* experimental hypoxia model.

Heart mitochondria were isolated as previously described (10). Briefly, 2 rats hearts were chopped in a mixture of 0.225 M mannitol, 0.075 sucrose, and 0.05 mM EDTA, pH=7.4 (MSE), 10 mg crystalline bacterial proteinase (Nagarase) and 0.05 ml of Tris buffer (1 M) was added to 5 ml of it and the chopped tissue was homogenized by a hand-operated glass homogenizer, diluted to 40 ml with more fresh MSE, centrifuged (8000 g, 10 min), whole pellet was rehomogenized and resuspended in 80 ml MSE, centrifuged (700 g, 10 min), supernatant removed and centrifuged (8000 g, 10 min) and brown pellet (mitochondrial fraction) was resuspended in 1.5 ml of MSE.

Protein measurements were performed according to the colorimetric method of Lowry (11). When needed, protein preparations were concentrated on Amicon Diaflo Y5.0 membranes at 800 p.s.i.

^{59}Fe (γ -emitter) and ^{32}P (β -emitter) quantitative radioactivity measurements were conducted in the dioxane LKB scintillation counting fluids using the LKB SK260 and the Wallac 410B liquid scintillation counters, respectively.

For the ^{59}Fe -related autoradiography of the isolated organelles, Fuji RX40 films were employed along with the Farrand XL transmission electron microscopy unit.

Estimations of magnesium stable isotopes (^{25}Mg , ^{24}Mg , and ^{26}Mg) were carried out in the Olivetti Prism DL600 isotope mass spectrometer suitable for studies on heterogenous samples of biological origin (5-8). For the PMC16 saturation with $^{25}Mg^{2+}$ cations, our original electro-osmotic technique has been applied (8, 9).

The iron-containing porphyrin monoadduct of fullerene C_{60} referred to as Porphylleren-MC16 or PMC16 (*buckminsterfullerene(C_{60})-2-(butadiene-1-yl)-tetra(o- γ -aminobutyryl-o-phthalyl)ferroporphyrin*) has been synthesized according to our modification of a conventional route proposed in (9, 12-14). Thus, diethyl phthalate was lithiated by butyllithium at $-78^{\circ}C$ followed by quenching carbanion with trimethylsilyl chloride. The resulting diethyl 3-(trimethylsilyl)phthalate was subsequently treated with butyllithium and DMF leading to the corresponding benzaldehyde. Its reaction with N-bromosuccinimide in the presence of Bu4NF gave diethyl 6-bromo-3-formylphthalate which is the final precursor for the substituted porphyrin synthesis. 5,10,15,20-Tetrakis[4-bromo-2,3-bis (ethoxycarbonyl)

phenyl]-21H, 23H-porphine was synthesized by Lewis acid-catalyzed condensation of this precursor with pyrrole followed by treatment with DDQ according to the standard Lindsay procedure. The Vilsmeier-Haack formylation of the obtained porphyrin E by DMF/POCl₃ mixture followed by Wittig reaction with allyltriphenylphosphonium bromide yielded butadienyl-substituted porphyrin F. Copper-catalyzed reaction of this porphyrin with the excess of γ -aminobutyric acid resulted in the formation of the 2-(buta-1,3-dienyl)-5,10,15,20-tetrakis[4-(3-carboxypropylamino)-2,3-bis (ethoxycarbonyl) phenyl]-21H,23H-porphine. Alkaline hydrolysis of this product, cation metathesis using MgCl₂, Diels-Alder reaction between butadienyl moiety and C₆₀ and metalation of porphyrin core with FeCl₂ finished the synthesis of the goal iron(II) 2-[1',4'-dihydrobenzo [60-fullerene-2'-yl]-5,10,15,20-tetrakis[4-(3-carboxypropylamino)-2,3-dicarboxyphenyl]porphyrinate tetramagnesium salt.

To identify the CS₂-extracted resulting product, the laser desorption-ionization (LDI) mass spectra were registered in Varian GT800 LC-MS machine and then processed in the HP6100-J2A analytical unit using a Sigma Delta Chem AX2000 data base.

For pharmacokinetic and autoradiographic studies, a special samples of [⁵⁹Fe]PMC16 (280-320 Ci/mmol) were obtained using the A grade ⁵⁹FeCl₂ (910-960 Ci/mmol, Obninsk Radiochemical Center of Russia) as a precursor.

A pure CS₂ was applied as a universal PMC16 extractant in studies on lyophilized samples of either isolated cell compartments or a crude heart tissue homogenates, 8.0-12.0 w/v, 22-25 °C, by extensive shaking. The extracts were repeatedly treated with 7.5 volumes pyridine (3x-5x); all post-extraction pyridine portions were then collected, combined, and concentrated in rotor evaporizer. A 15-20 μ l aliquots of the PMC16-containing concentrated extracts were fractionated by HPLC using a CosmoSil 5-PBB (the PentaBromBenzene-modified silica gel suitable for separation of porphyrinic fullerenes (15)) 20x250 mm column at 22 °C, 1,200-1,500 p.s.i., 10 ml/min, with a pure 1,2,4-trichlorobenzene as a mobile phase. The final PMC16 quantification was performed planigraphically with an automatized correction for molar extinction indexes once the elution profile got recorded by absorption at 180, 210, 320, and 470 nm (15), Perkin Elmer 266 QL HPLC Analytical System.

For the drug nano-size measurements as well as for the pH-dependent PMC16 cluster formation direct monitoring, a two-dimensional arrays of nanoparticles and their conglomerates were registered by the Atomic Force

Microscopy (AFM) in the Zelenograd-ERA M3 (Russia) AFM system (16). Apart of AFM, ²⁵Mg release and nanocluster formation and dissociation of [²⁵Mg]PMC16 nanoparticles within the eluent pH 5.0 - 9.5 range, two types of gel filtration systems were used: group separation with Sephadex G-10 and a 35x2.66 (i.d) cm glass column and fractionation with Sephadexes G-50 and G-75 and a 100x2.55 (i.d) cm glass column (8).

The PMC16-related Mg²⁺ release kinetics has been simultaneously tested, within the same pH range, by evaluation of Mg/Fe ratios using a routine flame atomic absorption spectrophotometry method. SANS (small angle neutron scattering) spectra of PMC16 monomers and dimers were registered and analysed in SANS 2TD accelerator at the International Nuclear Research Institute, Dubna, Russia, with a kind technical assistance provided by Dr. M.N. Osmolov.

For morphological tracing of PMC16 particles inside the organelle membranes, a metal-chelating iron response AFM toolbox (17) along with a simple imaging AFM biological version (18) were employed. The *in situ* morphology of mitochondria in myocardiocytes was observed by a transmission electron microscopy using our slight modification (Pt contrasting coating) of the previously described technique (19). A laser contrast confocal microscopy was additionally employed using a Nanofinder- S16E (Nanofinder Co., Russia) technology as described (9, 14).

Once mitochondria isolated, they were rapidly submitted to the Triton X-100 treatment (2.0%, v/v, +4 °C, 2 hrs, 10 mM tris-HCl pH 7.45) followed by extraction of a total pool of the low molecular mass compounds by addition of 10 volumes ice-cold acetone. The acetone-soluble material was then fractionated by our original HPLC procedure (ODS-S5CN stationary phase 10-60% linear pyridine gradient mobile phase, Altex 1800 15x280 mm column, 22 °C, 2,000 p.s.i., Gilson W100 UV-detecting HPLC system) in order to get both ATP/ADP ratio values and the ATP production rate estimated as γ [³²P]ATP c.p.m/mg protein (20). In all *in vivo* [³²P]orthophosphate ATP labelling tests, animals were sacrificed in 20-180 min time interval after a single 80-100 mCi/kg i.v. injection of the radioactive material. CK activity was measured as described earlier (7-8).

Both heart tissue homogenates and the isolated mitochondria samples were subjects for [O₂] consumption and [Δ H⁺] parameters estimation.

A Bio Rad OxyAnalyser SJ80 has been employed for the tissue/mitochondria oxygen consumption tests (21). In these studies, the phosphorescence-based oxygen analyzer was superior to the conventional oxygen electrode

system in that it provided an accurate, sensitive and reproducible quantitation of $[O_2]$. Measurements in this study were performed over periods up to 60 min, ensuring cell viability. Measurements on re-aerated suspensions showed that the probe was stable and did not interfere with cell function. Stoichiometric titration of the oxygen with ascorbate in the presence of ascorbate oxidase ($2 \text{ ascorbate} + O_2 \rightarrow 2 \text{ dehydroascorbate} + 2 H_2O$) was done as described (22).

The tissue free protons content was potentiometrically evaluated in homogenates using a Pt/Ar microelectrode in an extensive-aerated cell coupled with the $[O_2]$ detecting unit (9, 21).

Results

As shown in Figures 1 and 2, the PMC16 possesses an essential Mg^{2+} -carrying cationite potential. Noteworthy, the product behaves as a so called "smart nanoparticle" being capable to release magnesium exclusively in response to the pH acidic shift (Figure 2). At the same time, the PMC16 clusters formation is also found to be a

function of pH (Figures 2 - 4). These findings may be interesting in the case of myocardial hypoxia molecular pathogenesis, according to which a tissue acidosis is a direct and natural metabolic consequence of the hypoxia of any sort (1, 23). The acidosis induced release of $^{25}Mg^{2+}$ is what we may expect in case of the $[^{25}Mg]$ PMC16 *in vivo* administration. The amphiphilic character of this agent (9) is also in a favor to such expectations since the ambivalent solubility of the drug correlates normally with its membranotropic properties (2, 24, 25), and indeed, the PMC16 biomembrane uptake has been eventually found (Figure 5).

Both morphological and biochemical (Figure 6) patterns show a clear and positive effect of $[^{25}Mg]$ PMC16 on the hypoxia promoted myocardial cell energy metabolism disorders. Additionally, this has been proven by a high level of synergism manifested in the $[^{25}Mg]$ PMC16 hypoxia treated cases, i.e. by a synergism between the CK activity, ATP production rate, magnesium isotopes contents in the heart mitochondria, myocardial O_2 consumption and the extent of tissue acidosis ($[\Delta H^+]$) (Figures 7, 8).

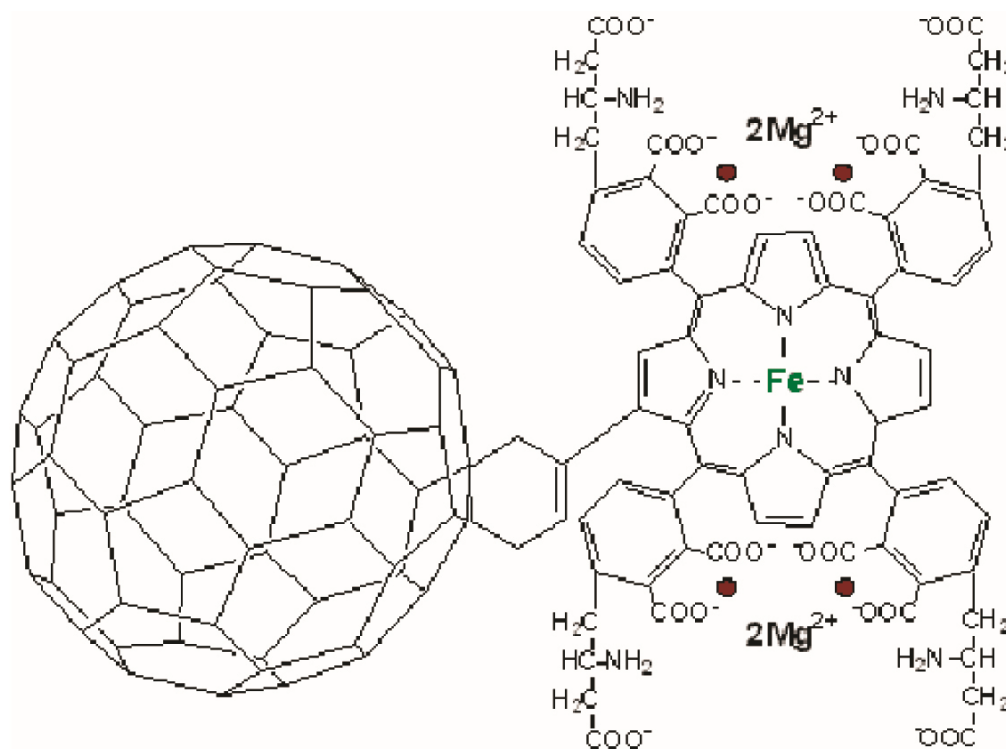


Figure 1. The PMC16 nanoparticles structure
Buckminsterfullerene(C60)-2-(butadiene-1-yl)-
-tetra(o- γ -aminobutyryl-o-phtalyl)porphyrin
 PORPHYLLEREN- MC16

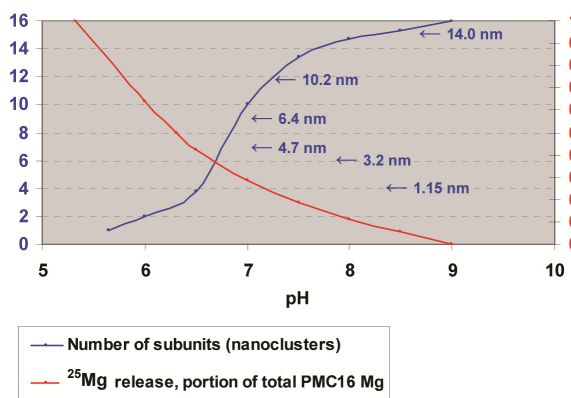


Figure 2. PMC16 cationite properties and nanoclusters formation as a function of pH.

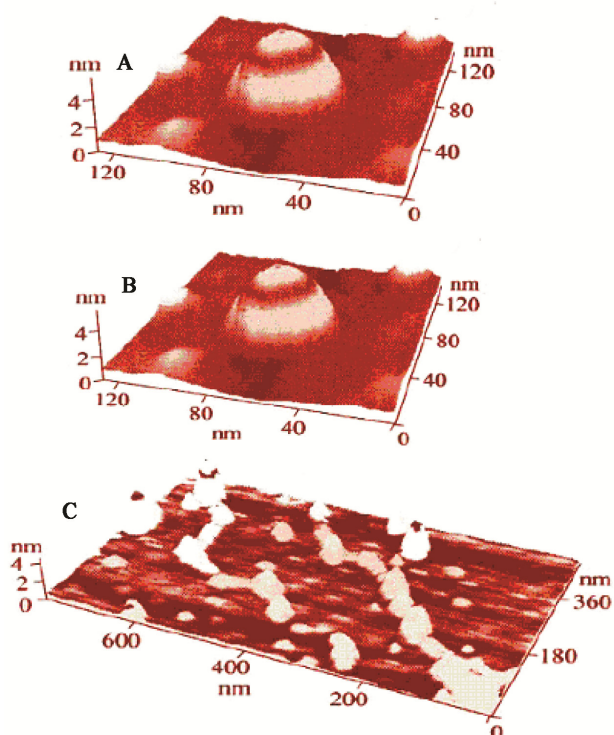


Figure 3. Laser contrast and AFM. PMC16 nanoclusters immobilized on acetyl cellulose membrane [26]. A) LCM, pH=7.00, B) LCM, pH=8.4, C) AFM, pH=8.8.

Another remarkable peculiarity of PMC16 nanoparticles is a fact of their days-long lasting retaining in the heart tissue (Figure 9) and, particularly, inside the heart mitochondria membranes (Figure 10).

A total lack of the PMC16 long-lasting “trapping” observed in tests conducted on several other tissues (liver, lungs, kidneys, skeletal muscles) is in accordance with the above stated assumption.

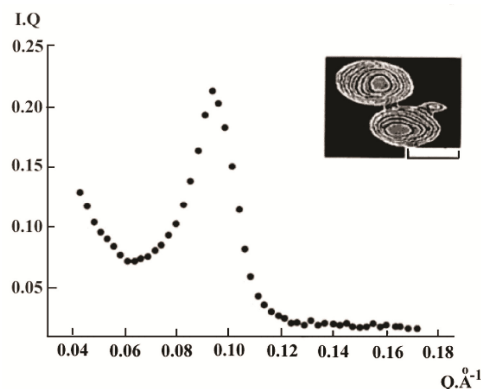


Figure 4. Small angle neutron scattering image of the PMC16 mono/dimer, pH 6.50 (scale bar, 1.0 nm)

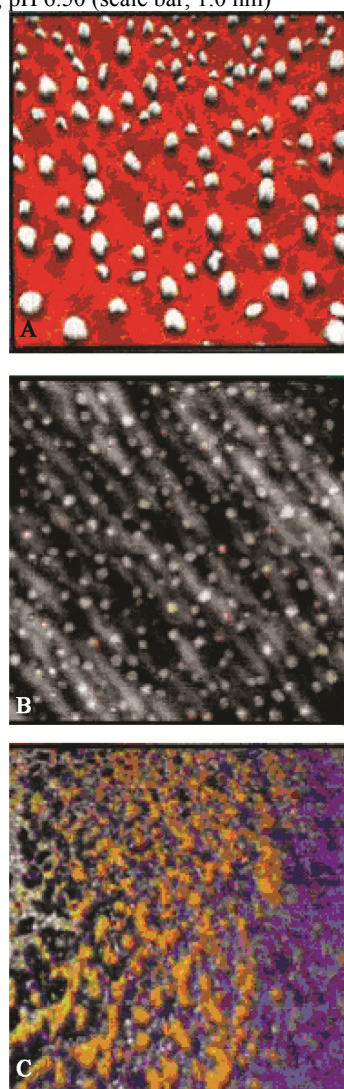


Figure 5. The PMC16 nanoparticles/clusters atomic force micrographs. A) Suspension, 400 mg/ml 1.5 mM K₂HPO₄ (pH 10.0), - 10 nm scale bar. B) Diaflo YM 1.0 membrane remained pellets, 400 mg/ml 1.5 mM K₂HPO₄ (pH 9.0) suspension used, - 100 nm scale bar. C) Rat myocardial mitochondria membrane lipid layer. 0.1 LD₅₀ PMC16, 10 hrs → 0.8 LD₅₀ DXR, 10 hrs, - 50 nm scale bar.

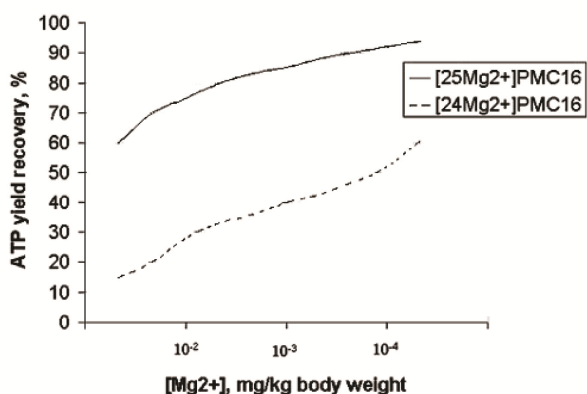


Figure 6. The effect of a PMC16-targeted delivery of Mg^{2+} on the DXR pre-suppressed ATP production in rat myocardium (0.8 LD₅₀ DXR i.v., 6 hrs → PMC16, i.v., 6 hrs).

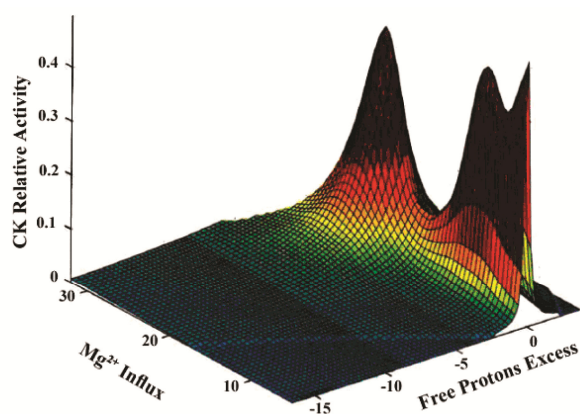


Figure 7. Synergism of the mitochondrial matrix CK activity, PMC16-related magnesium cations influx and the free protons excess degree. Isolated rat myocardial mitochondria pre-treated with 0.25 LD₅₀ PMC16.

A relatively fast systemic clearance of this nanomedicine along with a nearly perfect tissue clearance estimated for numerous PMC16 “non-trapping” tissues listed above (26) seems an additional argument to prove a high potential of PMC16 for the heart-selective $^{25}Mg^{2+}$ targeted delivery.

For more details on the PMC16 pharmacokinetics and biotransformation in rat, see report presented by Amirshahi et al. (26).

The “crescendo” of this segment of our work is the heart muscle targeted delivery of [^{25}Mg]PMC16 we have reached by developing of a special scheme of the multiple long-term administration of an extra low drug doses. In Figure 11, the true efficiency of this scheme (0.4 mg/kg, i.v. → [10 days] → 0.2 mg/kg, i.v. → [6 days] → 0.1 mg/kg, i.v. → ... up to 24 days monitored) is proven.

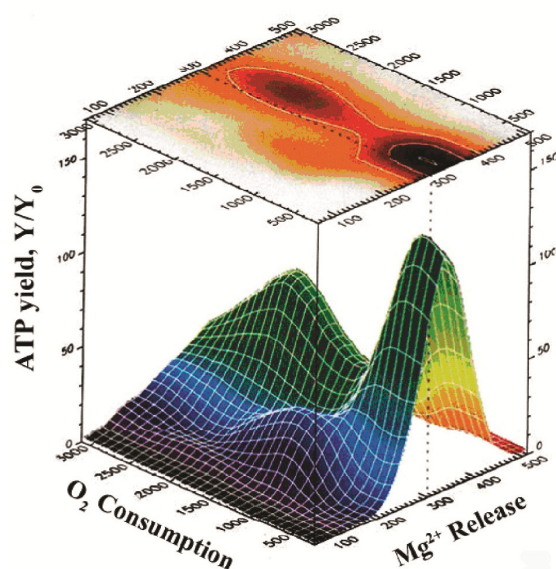
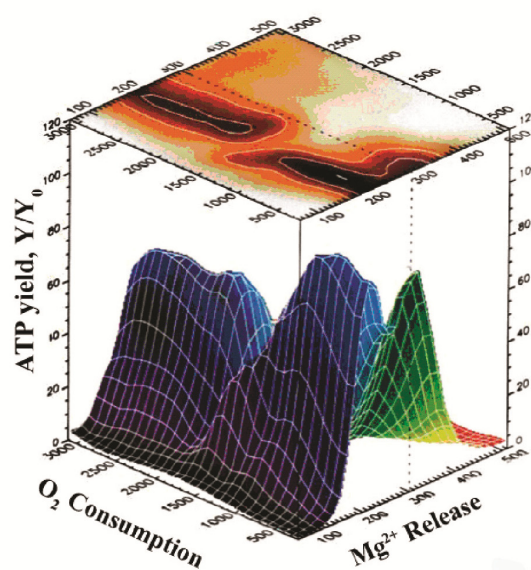


Figure 8. Synergism of ATP yield, oxygen consumption and the PMC16-related Mg^{2+} release in the rat heart muscle tissue (30 mg/kg PMC16, i.v., 12 hrs exposition). A) Zero spin magnesium test B) Magnetic magnesium test

The scheme proposed comes from our understanding of pharmacological meaning of the PMC16 heart muscle specific reception. Particularly, this scheme provides a *saturation* of majority if not of all of the heart-located PMC16 specific receptors in case of the gradual administration of drug doses *minimal but enough* to get this saturation reached. Meanwhile, all other receptor-lacking body compartments are not in a position to retain the drug as long as its concentration is below an accumulation-required elimination limit. That's the extra

low doses are for. All together, this creates a unique conditions for the heart drug targeting even *without any effort to manage the artificially designed targeted delivery path* like, for example, the external magnetic field navigation or the antibody involving liposome drug delivery (27-29, 25).

The above statements are supported by a complex and positive correlation revealed between the heart tissue ²⁵Mg content values and the tissue respiration parameters ([ATP], [ATP]/[ADP], Y/Y₀; [ΔO₂], [ΔH⁺]) measured in DXR-induced hypoxia chronic experiments (Figure 11).

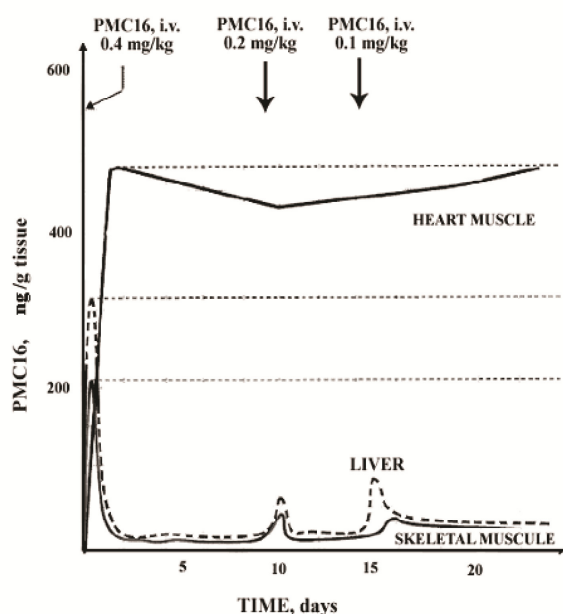


Figure 9. A highly selective targeting of PMC16 nanoparticles towards the rat heart muscle in a course of the long-term administration of an extra low drug dosage.

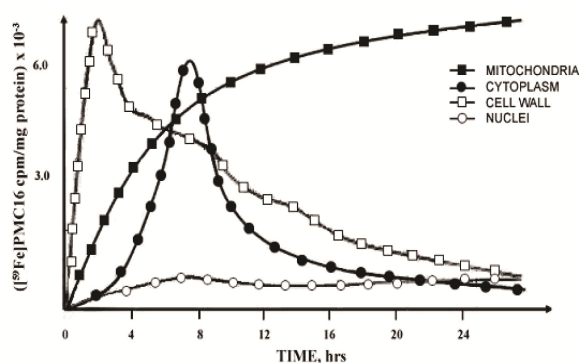


Figure 10. The heart muscle cell compartment retaining distribution of [⁵⁹Fe]PMC16 caused by a single i.v. administration in rats (30 mg/kg, 470-520 Ci/kg).

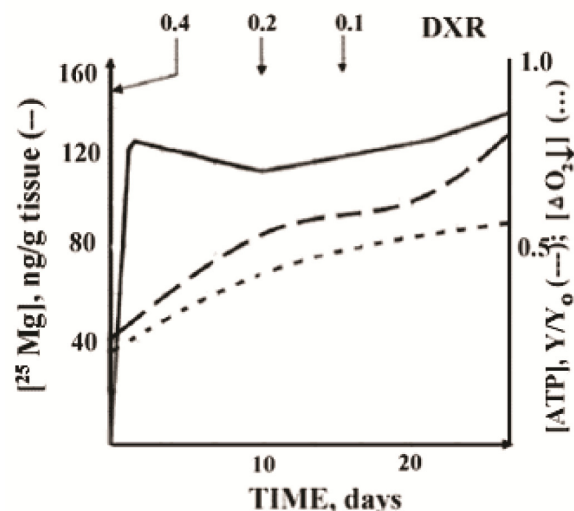


Figure 11. The rat myocardium tissue respiration affected by DXR in a course of [²⁵Mg²⁺]PMC16 administration (0.4 → 0.2 → 0.1 mg/kg i.v.). DXR, 80 mg/kg/24 hrs, i.v.

Discussion

The recent history of the medicinal use of fullerene-based nanoparticles includes a clear indication to their low acute toxicity (30, 24) as well as to a variety of data that reveals the fullerene autonomous cytostatic (31), immunosuppressant (32) and antioxidant (27) properties. It would be safe to say, however, that the main stream trends in a modern fullerenes nanopharmacology research deals with the targeted drug delivery problem due to a marked capabilities of these nanoagents to serve as a specific carriers for organic/bioorganic pharmaceuticals (28-29). As for a tissue targeting mechanism itself, magnetic and immuno-navigation paths *alone* were tested so far with respect to this very peculiar family of nanomedicines (27, 29, 30).

In the last, we have studied and reported the C₆₀-fullerene derivatives *cationite* activity (9). On other hand, this is exactly the activity needed to provide a delivery of ²⁵Mg²⁺ cations towards a hypoxia suffering cells and tissues. A targeted delivery may help to compensate the hypoxia-caused ATP losses owing to a known ²⁵Mg-related overactivation of both oxidative and substrate ADP phosphorylation paths of ADP in a cell (6-8).

The acidosis induced release of ²⁵Mg²⁺ is what we may expect in case of the [²⁵Mg]PMC16 *in vivo* administration. The amphiphilic character of this agent (9) is also in a favor to such expectations since the ambivalent solubility of the drug correlates normally with its membranotropic properties (2, 24, 25), and indeed, the

PMC16 biomembrane uptake has been eventually found (Figure 5).

DXR provides slight inhibitory effect towards ATP synthase and cytochrome oxidase in mitochondria (3, 9). The [^{25}Mg]PMC16 prophylactic or corrective use look promising to either prevent or correct the DXR-induced ATP-depletion and, to protect the heart muscle in general.

Noteworthy, the only reason why extra low doses of PMC16 are enough to promote an essential pharmacological effect in the hypoxia damaged myocardial cells, i.e. to promote a marked activation of the ATP synthesis, is the efficient delivery of ^{25}Mg isotopes known as the universal ATP production *overactivating agents* (5-9). So, despite a low tissue drug concentration, the energy metabolism rehabilitation is to be taken care of by a small amount of an *extremely active* ATP regeneration promoter which in the case of this study, is a magnetic magnesium isotope.

The data presented may serve as a background for a new nanopharmacological approach to prevent and correct myocardial hypoxic disorders. The way proposed includes the heart muscle targeted delivery of magnetic $^{25}\text{Mg}^{2+}$ isotope carrying by membranotropic cation-exchanging fullerene-based nanoparticles, PMC16. The heart targeting depends on the PMC16 tissue specific reception while the magnesium release is just a response to hypoxia-caused metabolic acidosis. That makes an agent tested a "smart medicinal nanoparticle". All findings listed look promising and requires further extensive studies.

Finally, the followings can be concluded from this study:

1) PMC16 is a low toxic membranotropic nanoparticle suitable for the heart muscle targeted delivery of $^{25}\text{Mg}^{2+}$ cations needed for the overactivation of ATP synthesis pre-suppressed in the DXR-induced hypoxia damaged myocardial cells.

2) Due to the PMC16-specific receptor located in the cardiomyocyte mitochondria membranes, a selective targeted delivery of the drug might be managed simply by a long term multiple administration of the drug extra low doses. This course may provide a prophylactic or therapeutic effect in medicinal hypoxic cardiotoxicity induced by DXR.

Acknowledgements

This work was kindly and totally supported by the Re-

mental Research Support Foundation (Moscow, Russia). The PMC16 synthesis and the nanoparticles $^{25}\text{Mg}^{2+}$ loading was performed owing to a technical assistance provided by the Division of Analytical Chemistry, La Sapienza University, Rome, Italy (Prof. L. Campanella) and by the Division of Organic Chemistry, M.V Lomonosov Moscow State University, Moscow, Russia (Prof. M.A. Yurovskaya). Special thanks to Dr. M. N. Osmolov, the International Nuclear Research Institute at Dubna, Russia, for his exceptional help in getting and analyzing the nanoparticles SANS images.

References

- Wallace KB, Starkov AA. Mitochondrial targets of drug toxicity. *Annu Rev Pharmacol Toxicol* 2000;40:353-88.
- Souid AK, Tacka KA, Galvan KA, Penefsky HS. Immediate effects of anticancer drugs on mitochondrial oxygen consumption. *Biochem Pharmacol* 2003;66(6):977-87.
- Wallace KB. Doxorubicin-induced cardiac mitochondrial onopathy. *Pharmacol Toxicol* 2003;93(3):105-15.
- Tokarska-Schlattner M, Wallimann T, Schlattner U. Multiple interference of anthracyclines with mitochondrial creatine kinases: preferential damage of the cardiac isoenzyme and its implications for drug cardiotoxicity. *Mol Pharmacol* 2002;61(3):516-23.
- Buchachenko AL, Kouznetsov DA, Arkhangelsky SE, Orlova MA, Markarian AA. Spin biochemistry: intramitochondrial nucleotide phosphorylation is a magnesium nuclear spin controlled process. *Mitochondrion* 2005;5(1):67-9.
- Buchachenko AL, Kouznetsov DA, Orlova MA, Markarian AA. Magnetic isotope effect of magnesium in phosphoglycerate kinase phosphorylation. *Proc Natl Acad Sci U S A* 2005;102(31):10793-6.
- Buchachenko AL, Kouznetsov DA, Arkhangelsky SE, Orlova MA, Markarian AA. Spin biochemistry: magnetic ^{24}Mg - ^{25}Mg - ^{26}Mg isotope effect in mitochondrial ADP phosphorylation. *Cell Biochem Biophys* 2005;43(2):243-51.
- Kouznetsov DA, Arkhangelsky SE, Berdieva AG, Khasigov PZ, Orlova MA. A novel electrophoretic technique designed to modify the ratio of magnesium isotopes inside the creatine kinase active sites. A preliminary report. *Isotopes in environmental and health studies* 2004;40(3):221-7.
- Tishkov VI, Varfolomeyev SD. Editors. [^{25}Mg]-Releasing nanoparticles for the ATP depletion correction in the hypoxia damaged myocardial cells. In: *Biocatalysis*; 2005, 26 June-1 July; Moscow -St. Petersburg, Russian Federation. Moscow: MSU Press; 2005.

10. Tyler DD, Gonze J. The preparation of heart mitochondria from laboratory animals. In: Estabrook RW, Pullman ME, editors. *Methods in Enzymology*. London: Academic Press Inc; 1967. p. 75-122.
11. Lowry OH. Protein measurement with the folin phenol reagent. *J Biol Chem* 1951;193(1):265-75.
12. Gouloumis A, Liu SG, Sastre A, Vazquez P, Echegoyen L, Torres T. Synthesis and electrochemical properties of phthalocyanine: fullerene hybrids. *Chemistry* 2000;6(19):3600-7.
13. Alonso CMA, Neves MGPMS, Tome AC, Silva AMS, Cavaliero JAS. Synthesis and Diels-Alder reactions of 2-(buta-1,3-dien-2-yl)-5,10,15,20-tetraphenylporphyrin. *Tetrahedron Letters* 2000;41(30):5679-84.
14. Hannink RHJ. *Nanostructure Control of Materials*. UK: CRC Press-Taylor & Francis; 2005.
15. Sidorov LN, Yurovskaya MA, Borshchevsky AY, Trushkov IV, Ioffe IN. *Fullerenes*. Russia: Examen Publications; 2005. (in Russian).
16. Schaefer DM, Reifengerger R, Patil A, Andres RP. Fabrication of two-dimensional arrays of nanometer-size clusters with the atomic force microscope. *Appl Phys Lett* 1995;66(8):1012-5.
17. Schmitt L, Ludwig M, Gaub HE, Tampé R. A metal-chelating microscopy tip as a new toolbox for single-molecule experiments by atomic force microscopy. *Biophys J* 2000;78(6):3275-85.
18. Fotiadis D, Scheuring S, Müller SA, Engel A, Müller DJ. Imaging and manipulation of biological structures with the AFM. *Micron* 2002;33(4):385-97.
19. Abrams GA, Bentley E, Nealey PF, Murphy CJ. Electron microscopy of the canine corneal basement membranes. *Cells Tissues Organs* 2002;170(4):251-7.
20. Kuznetsov DA, Govorkov AV, Zavijalov NV, Sibileva TM, Richter V, Drawczek JA. Fast estimation of ATP/ADP ratio as a special step in pharmacological and toxicological studies using the cell-free translation systems. *J Biochem Biophys Methods* 1986;13(1):53-6.
21. Vinogradov SA, Wilson DF. Metallotetrabenzoporphyrins. New phosphorescent probes for oxygen measurements. *J Chem Soc Perkin Trans II* 1995;2(1):103-111.
22. Lo LW, Koch CJ, Wilson DF. Calibration of oxygen-dependent quenching of the phosphorescence of Pd-meso-tetra (4-carboxyphenyl) porphine: a phosphor with general application for measuring oxygen concentration in biological systems. *Anal Biochem* 1996;236(1):153-60.
23. Waugh T, Telashima H. *Mitochondria*. 1st ed. Raleigh-Durham, NC: Research Triangle Publications; 2004.
24. Oberdörster G, Oberdörster E, Oberdörster J. Nanotoxicology: an emerging discipline evolving from studies of ultra-fine particles. *Environ Health Perspect* 2005;113(7):823-39.
25. Berdyshev TS, Shtark VL. Lipophilic xenobiotics in the tissue respiration medicinal control. In: Larin SS, Vazhankin OG, editors. *Perspectives in experimental pharmaceutical chemistry*. 1st edition. Novosibirsk - Tomsk - Moscow: Novosibirsk State University Press; 2004. p. 47-68. (in Russian).
26. European Patent Application EP1992339. Use of a magnesium isotope for treating hypoxia and a medicament comprising the same. [Online] 2008 Nov 19. Available from: URL:<http://www.freepatentsonline.com/EP1992339.html>
27. Malsch NH. *Biomedical Nanotechnology*. 1st ed. UK: CRC Press - Taylor & Francis Group; 2005.
28. Ravi Kumar MN. Nano and microparticles as controlled drug delivery devices. *J Pharm Pharm Sci* 2000;3(2):234-58.
29. Pankhurst QA, Connolly J, Jones SK, Dobson J. Application of magnetic nanoparticles in biomedicine. *J Phys D Appl Phys* 2003;36(13):R167-R81.
30. Hughes GA. Nanostructure-mediated drug delivery. *Nanomedicine* 2005;1(1):22-30.
31. Brigger I, Dubernet C, Couvreur P. Nanoparticles in cancer therapy and diagnosis. *Adv Drug Deliv Rev* 2002;54(5):631-51.
32. Freitas RA. What is nanomedicine? *Nanomed Nanotechnol Nanotechnol Biol Med* 2005; 1(1): 2-10.